

2012

# Using Surface Tension Gradients to Reduce Condensate Retention and Improve Heat Exchanger Performance in Air Conditioning Systems

Tyler J. Brest  
sommerad@muohio.edu

Khalid F. Eid

Andrew D. Sommers

Follow this and additional works at: <http://docs.lib.purdue.edu/iracc>

---

Brest, Tyler J.; Eid, Khalid F.; and Sommers, Andrew D., "Using Surface Tension Gradients to Reduce Condensate Retention and Improve Heat Exchanger Performance in Air Conditioning Systems" (2012). *International Refrigeration and Air Conditioning Conference*. Paper 1280.  
<http://docs.lib.purdue.edu/iracc/1280>

This document has been made available through Purdue e-Pubs, a service of the Purdue University Libraries. Please contact [epubs@purdue.edu](mailto:epubs@purdue.edu) for additional information.

Complete proceedings may be acquired in print and on CD-ROM directly from the Ray W. Herrick Laboratories at <https://engineering.purdue.edu/Herrick/Events/orderlit.html>

# Using Surface Tension Gradients to Reduce Condensate Retention and Improve Heat Exchanger Performance in Air Conditioning Systems

Tyler BREST<sup>1</sup>, Khalid F. EID<sup>1</sup>, Andrew D. SOMMERS<sup>2,\*</sup>

<sup>1</sup>Physics Department  
Miami University, Oxford, OH, 45056 USA  
Phone: (513) 529-1933, Fax: (513) 529-5629

<sup>2</sup>Department of Mechanical and Manufacturing Engineering  
Miami University, Oxford, OH, 45056 USA  
Phone: (513) 529-0718, Fax: (513) 529-0717

## ABSTRACT

This paper presents a novel method for patterning metal fin surfaces used in HVAC&R applications to mitigate problems associated with condensate retention. In this work, metallic surfaces are patterned to promote water droplet migration towards a specified region acting as a central drainage conduit. The surfaces were fabricated using photolithography, physical vapor deposition, and a surface-specific chemical coating and then characterized using spray (fine mist) testing and small droplet (2-10  $\mu\text{L}$ ) injection via microsyringe. In this study, we have also analyzed the effect of the chemical treatment on the observed wettability change (i.e. the degree of transformation of our surfaces from hydrophilic to hydrophobic). The impact of surface tension gradients was also explored by analyzing the deformation and asymmetry of droplets on such surfaces. Results from these tests have shown a significant ( $30^\circ$  -  $40^\circ$ ) increase in the static contact angle and severe deformation of droplets due to these surface gradient patterns on the surface. These preliminary results suggest that micro-structural patterning could be used to help reduce condensate retention on metallic fins.

## 1. INTRODUCTION

The motivation for this project stems from the application of heat exchangers in heating, ventilation, air-conditioning and refrigeration (HVAC&R) systems. Current designs make extensive use of copper and aluminum surfaces which are naturally hydrophilic. Because of this intrinsic property, water is likely to condense and adhere to these surfaces in the form of water droplets when the system is operating below the dew point temperature. Ordinarily, this water will continue to build on the surface until it is removed by gravity or the air-flow passing through the system. Water condensation can be problematic in these systems for a number of reasons. Water retention often leads to decreased heat transfer performance and increased air-side pressure drop. In refrigeration systems, water retention leads to ice formation and shorter defrost intervals. The net result is a decrease in the overall efficiency of these systems. This research is therefore aimed at developing new techniques which can be applied to metallic surfaces to help mitigate these issues. More specifically, the goal of this research is to produce non-homogenous, chemically-modified aluminum and copper surfaces to more effectively manage and remove condensed water on heat transfer surfaces.

The most common approach to this problem is the use of a homogenous chemical coating to decrease the wettability of the surface. This behavior can be seen in nature through the numerous, naturally occurring ways that plants and animals repel water (Sharma *et al.*, 2011, Feng *et al.*, 2007). While this would certainly decrease water retention on these surfaces, a homogeneously coated surface would permit (even facilitate) condensate carryover into the occupied space which could give rise to several additional concerns as well as biological hazards (Puckorius and Thomas, 1995). In HVAC&R applications, controlling the direction of condensate movement on the surface is often as important as the physical removal of those droplets. Therefore, a surface with a patterned anisotropic wettability may be preferred since droplet motion can be restricted to one direction—namely, downward with gravity. Previous work has shown that anisotropic surfaces can be created using photolithography and chemical treatment. For

---

\* Assistant Professor, corresponding author, e-mail: [sommerad@muohio.edu](mailto:sommerad@muohio.edu)

example, Sommers and Jacobi (2006) demonstrated that aluminum surfaces with anisotropic micro-scale topographical features can be used to manipulate the critical droplet size and affect the overall wettability. Furthermore, if a gradient exists on the surface, then a net surface tension force is produced that tries to move the droplet in the direction of the gradient. This could then be used to help move water droplets to a desired location on the fin surface. Adding both the effects of an anisotropic wettability and a surface tension gradient is predicted to lead to a significant reduction in the overall retention of water on heat exchangers used in HVAC&R systems.

Surface tension gradients have been applied everywhere from hydrodynamics to the herding of bacteria (Fauvart et al., 2012). Induced droplet motion was first reported by Chaudhury and Whitesides (1992) who applied a chemical surface tension gradient on a solid silicon substrate. With this gradient, they were able to create droplet motion on a horizontal plate tilted upwards to  $15^\circ$ . This was important as they explained that droplet motion required contact angle hysteresis  $\theta < 10^\circ$ . Improvements were made by Daniel et al. (2001) who showed a displacement velocity of 0.15-1.5 m/s for a 0.1-0.3 mm diameter droplets using the same approach as Chaudhury and Whitesides but arranged the gradient radially rather than linearly. Daniel and Chaudhury (2002) determined that the droplet velocity was also related to the contact angle hysteresis which affected the surface tension (Clegg, 2011). They also found that the measured velocities were linearly proportional to the droplet radius. These gradient surfaces were all created using a continuous chemical deposition method described by Elwing et al. (1986) which could not be used here. (In this study, the surface tension gradients were created by linearly varying the spacing of parallel microchannels / microstripes on the surface. It was thought that this geometry would not only facilitate improved drainage but may also better resist condensate carryover.) Many studies have also been published on the modeling of droplet behavior in both static and dynamic contexts; however, most of these works have been concerned with homogeneous surfaces (i.e. El Sherbini, 2003; Dussan, 1985; Vranken et al., 2010; Patankar et al., 2005; Brakke, 1992).

In summary, this study which builds upon earlier research on the topic describes a relatively inexpensive method for manufacturing anisotropic fin surfaces and managing condensate on the fin surface of heat exchangers. To date, photolithography, metal deposition, laser etching, and micro-milling techniques have all been explored as means of creating these micro-scale gradient geometries. In this study, photolithography was used to selectively deposit a thin layer of aluminum on a copper surface to create the gradient pattern. A hydrophobic self-assembled monolayer (i.e. heptadecafluoro-1-decanethiol) was then used to reduce the surface energy of the copper to form alternating regions of increased hydrophobicity and hydrophilicity. A ramé-hart goniometer was used to measure the local static contact angle of water droplets placed on these modified surfaces, and a high-resolution CCD camera was used to determine the location of these measurements with high accuracy. Our initial results have shown that the surface tension gradient on these surfaces not only affects the local contact angle in a way that is consistent with the underlying surface tension force, but these surfaces also promote the collection of water in preferred regions on the surface. The results from this work are expected to provide guidance in the design and development of advanced heat transfer surfaces for use in high-efficiency air conditioning systems.

## 2. EXPERIMENTAL METHODS

### 2.1 Sample Fabrication


Our research utilizes a two-step technique developed by Saunders *et al.* (2007) where a metallic surface is roughened to increase surface area, and then submerged in a solution containing heptadecafluoro-1-decanethiol (HDFT) to grow a self-assembled monolayer (SAM). Starting with a Cu block with a polished surface, the first step is to immerse the block in an AgNO<sub>3</sub> solution for 2 minutes to create a silver-coated Cu surface with significant nanoscale roughness. Following this step, the sample is rinsed in deionized (DI) water, sonicated in an ultrasonic bath for 1 minute, and dried by nitrogen gas. Next, the sample is immersed in the HDFT solution (diluted in dichloromethane) for six minutes and rinsed. The HDFT SAM is hydrophobic due to its non-polar bond. Thus, the static contact angle increases from approximately  $90^\circ$  for the original polished Cu surface to  $130^\circ$  for the rough, Ag-coated surface. (If the roughening step is not performed, the static contact angle following immersion in the HDFT increases to only approximately  $110^\circ$ .)

When trying this process on aluminum, we noticed that the contact angle did not change appreciably from its original value of just below  $90^\circ$  following immersion in the HDFT solution. Capitalizing on this discovery, we then fabricated Al microchannels on a polished Cu surface (using metal deposition techniques) and immersed the samples

in HDFT which caused the Cu stripes to become more hydrophobic while the Al stripes remained mildly hydrophilic. The relative width of the alternating Al and Cu stripes was varied smoothly so as to create a surface tension gradient on the surface. The aim of the gradient was to create a directional force that would act on the water droplets and cause them to move along the gradient direction. Furthermore because the Al stripes would be preferentially wetted more than the Cu stripes, it was expected that the three-phase contact line of the droplets would be highly distorted from the typical circular/elliptical shape.

Standard photolithography was used to fabricate the Al stripes, where a lift-off resist (LOR)/S1813 bilayer was used to pattern Al stripes of thickness 150 nm on a polished Cu block. After lift-off in 1165 remover, the sample was immersed for 6 minutes in HDFT diluted in dichloromethane and rinsed for 2 minutes in dichloromethane and then finally dried using nitrogen gas. (Note: The samples reported in this work were not pre-roughened using AgNO<sub>3</sub>.) Table 1 shows the spinning, baking, and exposure parameters used in this work. Our finished surface was a 3 x 3 inch copper square containing nine 1 x 1 inch aluminum/copper striped patterns as shown in Fig. 1.

**Table 1** Standard photolithographic process as performed on Cu plates

| Photoresist | Spinning             | Soft Bake       | Exposure   | Developer    |
|-------------|----------------------|-----------------|--|--------------|
| LOR         | 40 sec @<br>3000 rpm | 150°C<br>10 min |  |              |
| S1813       | 40 sec @<br>4000 rpm | 105°C<br>1 min  | 10 seconds   | 40 sec CD-26 |

|  |  |   |
|--|--|---|
| Single Gradient<br>for 4 mm<br>diameter<br>droplet | Single Gradient<br>for 8 mm<br>diameter<br>droplet | Single Gradient<br>for 12 mm<br>diameter<br>droplet |
| Double<br>Gradient<br>300/10 µm                    | Double<br>Gradient<br>200/10 µm                    | Double<br>Gradient<br>100/10 µm                     |
| Bare<br>homogenous<br>baseline Al<br>surface       | Triangular<br>Pattern<br>1:2 base to<br>length     | Triangular<br>Pattern<br>3:10 base to<br>length     |

**Fig. 1** Layout of various individual patterns on photomask/sample

## 2.2 Sample Characterization

A Rame-Hart precision goniometer was used to obtain information about the prepared surfaces by analyzing both the static and dynamic contact angles (i.e. advancing and receding angles) formed by water droplets on the surface. The apparent contact angle is the angle formed between the droplet and the surface in a static situation (usually a horizontal orientation). Advancing angles are determined by slowly injecting water into a droplet on the surface using a microsyringe and then measuring the contact angle that is formed when the droplet first begins to move (or advance) on the surface. The angle that is formed with respect to the surface just before the droplet advances is referred to as the advancing contact angle. Likewise the same process is used to capture the receding angle; we draw

water from the droplet into the microsyringe until the droplet recedes along the surface. The angle that is formed just before droplet recession is referred to as the receding contact angle. Once these measurements have been performed, then the difference between the advancing and receding angles (or the droplet hysteresis) can be calculated. Generally speaking, the lower the contact angle hysteresis is, the more hydrophobic the surface is. Thus, reduced water retention is usually associated with surfaces of low contact angle hysteresis. Coupled with the goniometer for contact angle measurement, a CCD camera was placed above the sample in order to accurately determine the droplet location on the surface and to check for consistency and gradient performance. Logistically speaking, this was done by taking a picture of the droplet with the overhead camera and then using a standard imaging software package (KAPPA ImageBase) to measure the distance of the droplet from a fixed edge.

We also used the spray test method to analyze the preferential location of droplets on our patterned surfaces. After applying a fine mist to the sample from a nonbiased direction, the resulting droplet distribution was examined using an optical microscope. These tests proved extremely helpful in determining the effect that our patterns had on droplet behavior (including deformation due to interaction with the gradient surface).

### 2.3 Surface Tension Modeling

If we take a water droplet on a horizontal surface, the net surface tension force along any direction is zero. However, if we create a surface tension gradient, then the contributions from the two ends of the droplet will not completely cancel out. This results in a net surface-tension-gradient force that tries to move the droplet in the direction of the gradient (i.e. in the  $x$ -direction). Perhaps more importantly, this surface-tension-gradient force could be used to potentially facilitate the removal of small droplets from a surface and/or droplet movement on a flat horizontal surface.

So how strong of a gradient would be needed to move a droplet on a horizontal surface? To begin, let us consider a simple circular droplet that is deformed due to the existence of an underlying gradient. If the gradient was not present, this droplet would exist as a spherical cap as shown in Fig. 2.



**Fig. 2** Schematic of a droplet on a (a) homogeneous surface, and (b) a surface with an underlying gradient

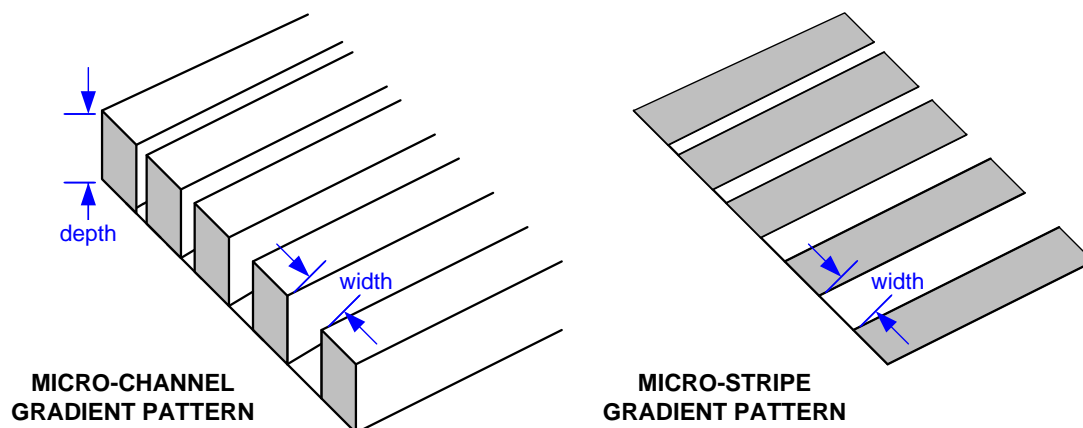


**Fig. 3** Two possible linear surface tension gradient designs (single gradient pattern shown). In the double gradient design (not shown), both widths are systematically varied.

Now let's consider a simple case where the local contact angle of a droplet on a horizontal surface does vary from one end of the droplet to the other due to the presence of a gradient (see Fig. 3) such that:

$$\cos \theta(x) = a_1 x^3 + a_2 x^2 + a_3 x + a_4 \tag{1}$$

where

$$\cos \theta(0) = \cos \theta_{max} \tag{2a}$$

$$\cos \theta(D) = \cos \theta_{min} \tag{2b}$$

$$\left. \frac{d(\cos \theta)}{dx} \right|_{x=0} = \psi \tag{2c}$$

$$\left. \frac{d(\cos \theta)}{dx} \right|_{x=D} = \psi \tag{2d}$$

as shown in Fig. 4. Using these boundary conditions to solve for the constants, one finds that

$$\cos \theta(x) = -\frac{2}{D^3} \left[ (\cos \theta_{min} - \cos \theta_{max}) - \psi D \right] x^3 + \frac{3}{D^2} \left[ (\cos \theta_{min} - \cos \theta_{max}) - \psi D \right] x^2 + \psi x + \cos \theta_{max} \tag{3}$$

The surface tension force associated with this droplet deformation can be calculated using the equation:

$$F_s = -\gamma D \int_0^\pi \cos \theta \cos \phi \, d\phi \tag{4}$$

$$F_s = -\gamma D \int_0^\pi (a_1 x^3 + a_2 x^2 + a_3 x + a_4) \cos \phi \, d\phi \tag{5}$$

Substituting  $x = R(1 - \cos \phi)$  into this expression and integrating yields

$$F_s = -\gamma D \left[ \frac{-15\pi}{8} a_1 \left(\frac{D}{2}\right)^3 - \pi a_2 \left(\frac{D}{2}\right)^2 - \frac{\pi}{2} a_3 \left(\frac{D}{2}\right) \right] \tag{6}$$

$$F_s = \gamma D \left[ \frac{9\pi}{32} (\cos \theta_{min} - \cos \theta_{max}) - \frac{\pi D}{32} \psi \right] \tag{7}$$

If the variation of the contact angle is linear as shown, then  $\psi = (\cos \theta_{min} - \cos \theta_{max}) / D$ . In this case, the surface tension force equation simplifies to:

$$F_s = \frac{8\pi}{32} \gamma D \left[ \cos \theta_{min} - \cos \theta_{max} \right] \tag{8}$$

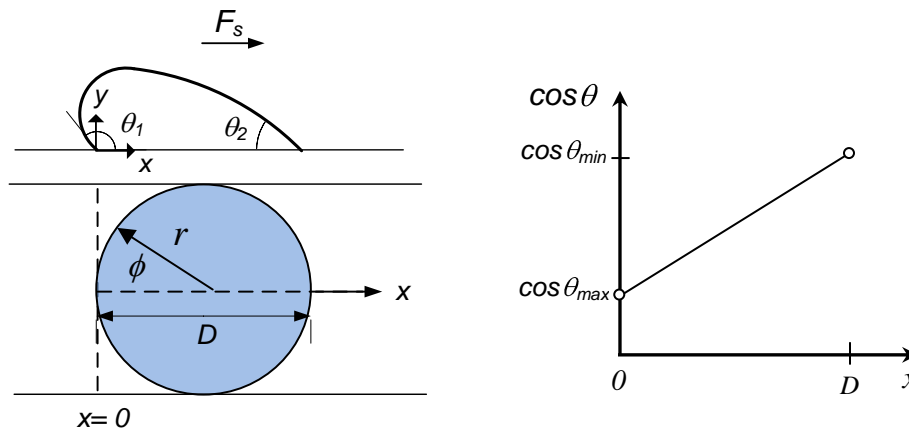


Fig. 4 Possible contact angle variation due to a surface tension gradient

So how does this compare to published expressions for the surface tension force on a surface? According to El Sherbini (2003), the surface tension force on a homogeneous surface can be represented as:

$$F_s^* = \frac{24}{\pi^3} \gamma D \left[ \cos \theta_{rec} - \cos \theta_{adv} \right] \quad (9)$$

In the case where the droplet is moving (i.e.  $\theta_{max} = \theta_{adv}$  and  $\theta_{min} = \theta_{rec}$ ), then these two expressions yield nearly the same value. Moreover, the leading coefficient in these expressions (referred to as the retentive force factor,  $k$ ) depends on the shape of the droplet base contour as well as the variation of the contact angle. Various values for  $k$  have been suggested (Dussan and Chow, 1983; Extrand and Gent, 1990; Extrand and Kumagai, 1995). This simple analysis, however, does show that for a droplet to move on a flat surface, it must be able to overcome the contact angle hysteresis.

## 2.4 Design of a Surface Tension Gradient

The ideal for our gradient is to facilitate movement and growth of water droplets on metal during condensation. Thus, if we start with the Wenzel model of wetting (which assumes  $\theta < 90^\circ$ ), we should be able to derive an expression that could be used when designing a surface tension gradient for droplet movement. In the Wenzel's model, the new apparent contact angle  $\theta^*$  is related to the original contact angle  $\theta$  through a roughness factor  $r$  such that

$$\cos \theta^* = r \cdot \cos \theta \quad (10)$$

where  $r$  is the area fraction of the liquid/solid contact (i.e. wetted area over the projected area). (Note: In this model,  $r \geq 1$ .) Now, let's consider a small circular droplet sitting atop a horizontal surface patterned with a surface wettability gradient and assume that half of the droplet is characterized by the advancing contact angle and half of the droplet is characterized by the receding angle to simplify analysis. This approach has been used by others including Dimitrakopoulos and Higdon (2001). Using Wenzel's model then to predict the advancing and receding contact angles, we can write the surface tension force on a micro-structured (or, micro-stripped) gradient surface as:

$$F_s = -\gamma D \int_0^{\pi/2} r \cos \theta_{rec} \cos \phi \, d\phi - \gamma D \int_{\pi/2}^{\pi} r \cos \theta_{adv} \cos \phi \, d\phi \quad (11)$$

Let's further assume that the surface tension gradient varies linearly such that

$$r = r_o + \frac{dr}{dx} x = r_o + \frac{dr}{dx} R (1 - \cos \phi) \quad \text{where} \quad (12a)$$

$$r = r_o \quad \text{for } \phi = 0^\circ \quad (12b)$$

$$r = r_o + \frac{dr}{dx} 2R \quad \text{for } \phi = 180^\circ \quad (12c)$$

Substituting and simplifying,

$$F_s = -2 \gamma R \cos \theta_{rec} \left[ r_o + \frac{dr}{dx} R \left( 1 - \frac{\pi}{4} \right) \right] + \pi \gamma R^2 \cos \theta_{adv} \frac{dr}{dx} + 2 \gamma R \cos \theta_{adv} \left[ r_o + \frac{dr}{dx} R \left( 1 - \frac{\pi}{4} \right) \right] \quad (13)$$

Here if  $F_s \neq 0$  then the droplet should move on the horizontal surface. Therefore, the minimum surface tension gradient necessary for droplet movement on a flat surface is found by setting  $F_s$  equal to zero and solving for  $dr/dx$  which results in

$$\frac{dr}{dx} = \frac{r_o (\cos \theta_{rec} - \cos \theta_{adv})}{R \left[ \left( 1 + \frac{\pi}{4} \right) \cos \theta_{adv} - \left( 1 - \frac{\pi}{4} \right) \cos \theta_{rec} \right]} \quad (14)$$

A few observations can be gleaned from this expression. First, the surface tension gradient scales directly with the contact angle hysteresis. In other words, the larger the underlying hysteresis is, the large the gradient needs to be to overcome it. Second, the gradient is proportional to the initial roughness factor,  $r_o$ . Larger gradients are needed in cases of large initial roughness factors. Third, the surface tension gradient is inversely proportional to the droplet

radius,  $R$ . This is because as the droplet radius increases, there is more distance for the contact angle to change. Thus, the necessary rate of change of the roughness factor (and hence the surface tension gradient) gets smaller as the droplet size gets larger. Finally, the gradient is smaller on surfaces with large advancing contact angles and larger on surfaces with small receding contact angles. (i.e. Droplets are more likely to move on surfaces with large advancing angles, whereas droplets are less likely to move on surfaces having small receding contact angles.) Note: The advancing and receding contact angles are key measurements that characterize the hydrophobicity or hydrophilicity of a surface (Oner and McCarthy, 2000; Hsieh *et al.*, 1995; Yerushalimi-Rozen *et al.*, 2004; Walzel *et al.*, 2005).

### 3. RESULTS AND DISCUSSION

#### 3.1 Static Droplets

After performing a spray test and then imaging the surface, we see droplets (1-5 $\mu$ L) that are significantly distorted from the typical circular base contour shape as they span multiple stripes on a linear gradient surface as shown in Fig. 5. This image shows the extreme corrugation of the droplet contact line, the “pinning” of droplets at the edge of the copper regions, and the elongation of droplets. Furthermore, it can be seen that the droplet is preferentially wetting the hydrophilic Al stripes which appear to exhibit static contact angles characteristic of aluminum. Likewise, the portions of the contact line spanning a copper stripe reflect the much higher contact angles characteristic of copper coated with HDFT. (Note: The data presented here are for samples that were not pre-roughened using AgNO<sub>3</sub>. Thus, we might have expected to see static contact angles of approx. 90° for droplets resting on the aluminum-coated regions of the surface and contact angles of 110° – 120° for droplets resting on the HDFT-coated copper regions.) Sections of the droplets oriented parallel to the stripes also clearly demonstrate the “pinning effect” that occurs due to this sharp and abrupt contrast in hydrophobicity. For example, if a droplet on an aluminum stripe is pinned by the beginning of a copper stripe, the droplet will not spill onto the copper until a contact angle higher than that of copper is reached. This effect is demonstrated more convincingly by the extreme shape distortion of the droplets in Fig. 5a. As droplets from the sprayed mist come in contact with the surface, they show a clear tendency to stick to the aluminum sites but roll over the copper sites until they find aluminum. This interaction allows droplets to fully occupy the triangular areas as shown in Fig. 5b.

#### 3.2 Dynamic Droplets

Based on our earlier modeling work, we initially expected to see some droplet motion on our gradient surfaces (albeit on the order of millimeters). Despite a lack of motion, we were able however to observe the preferential expansion of droplets in one direction as they were injected onto the surface. Figure 6 shows an image captured using our goniometer software, which reveals how a 5  $\mu$ L droplet ‘leans’ in the preferred direction (to the right) but does not experience any motion. Increasing the volume of the droplet by injecting it with more water would further show the droplet expanding to the right.

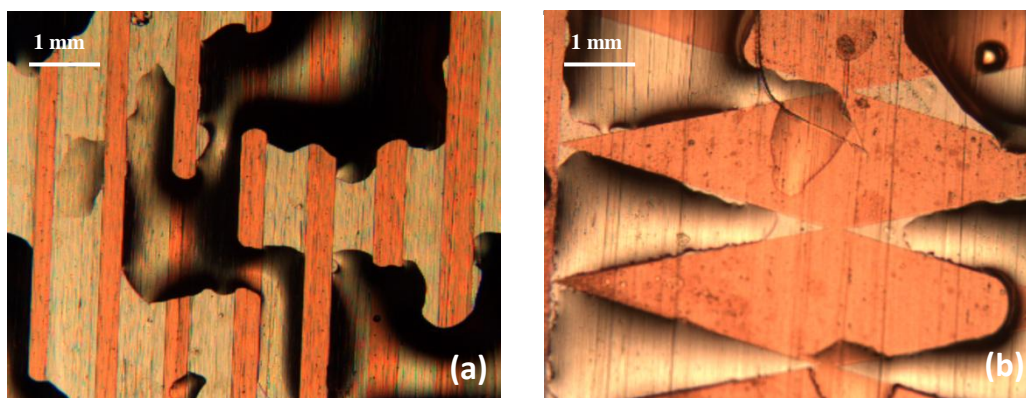


**Fig. 5** Spray test images showing distorted droplets on a (a) linear gradient surface, and (b) triangular gradient surface where the copper regions are hydrophobic



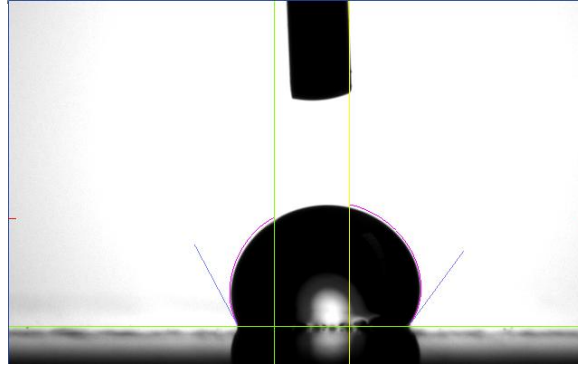


**Fig. 6** Image of an injected droplet (5  $\mu\text{L}$ ) on a gradient surface

Based on these results, we then examined the contact angles of droplets placed at different locations on a gradient surface. We had concluded that a droplet placed on an increasingly cupreous part of a gradient surface should reflect an increasing static contact angle. Given that the gradient pattern repeated itself 4 to 5 times on the surface, we thus expected to see the static contact angle decrease gradually and then increase abruptly as we moved from one gradient region to the next. Figure 7 shows the data collected for this test along with a visual representation of our surface. Although we expected to see a saw-tooth pattern restarting at each gradient boundary with the contact angle decreasing from left to right, such a conclusion was simply not possible with this initial set of data due to the uncertainty of these measurements. Follow-up testing is currently underway.

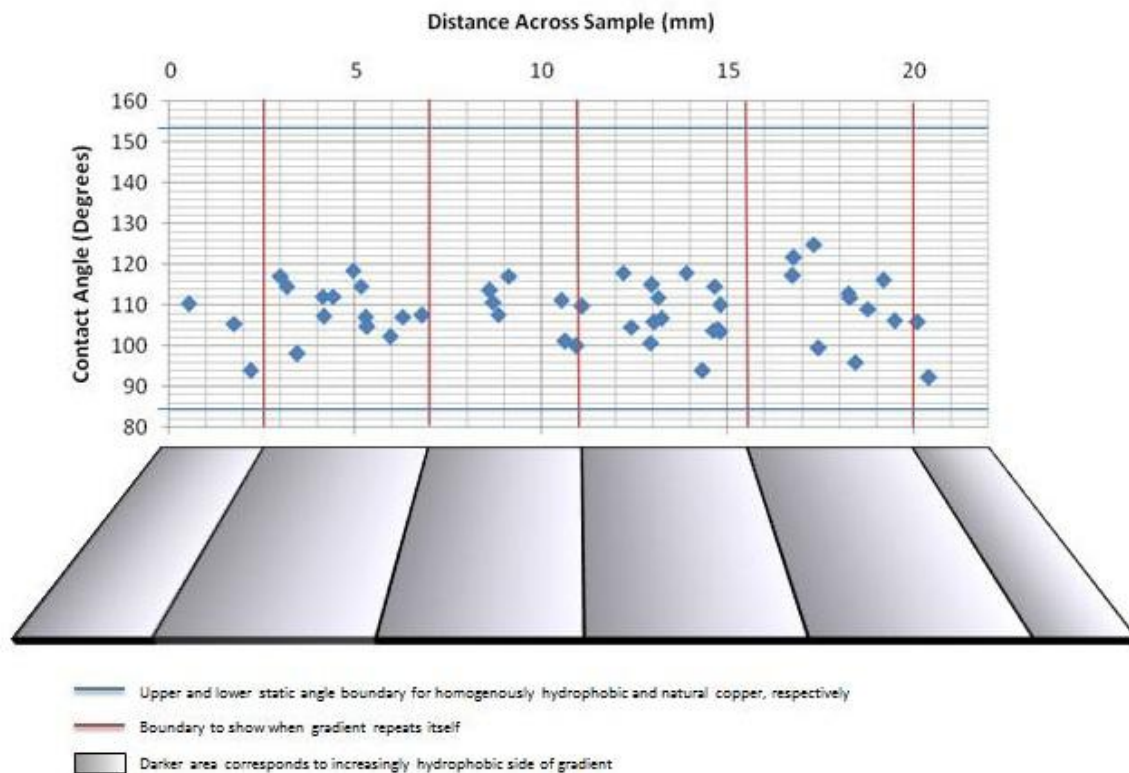


**Fig. 7** Measured static contact angle data on a linear gradient surface

#### 4. CONCLUSIONS

In this study, a method of manufacturing surface tension gradients on aluminum and copper substrates was explored. More specifically, surfaces were fabricated using photolithography, physical vapor deposition, and a surface-specific self-assembled monolayer (SAM). Following their manufacture, surfaces were characterized by spray testing and small droplet (2-10  $\mu\text{L}$ ) injection via microsyringe. The deformation and asymmetry of droplets on these surfaces were also studied. Although movement of individual droplets was not observed, the results from these tests revealed a significant ( $30^\circ - 40^\circ$ ) increase in the static contact angle coupled with significant droplet deformation due to the existence of the underlying surface tension gradient. Spray testing on surfaces in a horizontal orientation have also shown that the surface tension gradient on these surfaces not only affects the local contact angle in a way that is consistent with the underlying surface tension force, but these surfaces also promote the collection of water in preferred regions on the surface (i.e. regions of high hydrophilicity). Modeling work was also undertaken to examine the potential impact and design of using surface tension gradients in real systems. The results from this study (especially the spray testing images) suggest that these ideas could be beneficial in a variety of air-cooling applications where both heat and mass transfer occur.

#### NOMENCLATURE

|          |                       |              |        |                         |
|----------|-----------------------|--------------|--------|-------------------------|
| $D$      | Droplet diameter      | (mm)         | $\psi$ | Gradient rate of change |
| $F_S$    | Surface tension force | (N)          | $x$    | Distance (mm)           |
| $\phi$   | Azimuthal angle       | ( $^\circ$ ) |        |                         |
| $\gamma$ | Surface tension (N/m) | ( $^\circ$ ) |        | <b>Subscripts</b>       |
| $r$      | Roughness factor      | (--)         | adv    | Advancing               |
| $\theta$ | Contact angle         | ( $^\circ$ ) | red    | Receding                |

#### REFERENCES

- A.I. El Sherbini, 2003, Modeling Condensate Drops Retained on the Air-Side of Heat Exchangers, Ph.D. thesis, University of Illinois at Urbana-Champaign, Urbana, IL.
- A.I. El Sherbini, A.M. Jacobi, 2004, Liquid drops on vertical and inclined surfaces: II. A method for approximating drop shapes, *J. Colloid Interface Sci.* 273: 566-575.
- Brakke K. A., 1992, "The surface evolver", *Experimental Mathematics*, 1, 2: 141-165.
- Clegg, C., Static contact angle is not always enough. 2011. Rame Hart Instrument Co. Newsletter.
- Chaudhury, M.K., Whitesides, G.M., 1992, How to make Water Run Uphill, *Science*, 256: 1539-1541.
- Chen W, Fadeev A Y, Hsieh M C, ner D, Youngblood J and McCarthy T J, 1995, Ultrahydrophobic and ultralyophobic surfaces: some comments and examples, *Langmuir*. 15: 3395-3399.
- Chen Y, He B, Lee JH, Patankar NA, 2005, Anisotropy in the Wetting of Rough Surfaces, *Journal of Colloid and Interface Sci.*, 281: 458-464.
- Daniel, S., Chaudhury, M.K., 2002, Rectified Motion of Liquid Drops on Gradient Surfaces Induced by Vibration, *Langmuir*, 18: 3404-3407.
- Daniel, S., Chaudhury, M.K., Chen J.C., 2001, Fast Drop Movements Resulting from the Phase Change on a Gradient Surface, *Science*, 291: 633-635.
- Dimitrakopoulos, P., Higdon, J.J.L., 2001, On the Displacement of Three-Dimensional Fluid Droplets Adhering to a Plane Wall in Viscous Pressure-Driven Flows, *J. Fluid Mechanics*, 435:327-350.
- Dussan V., E.B., Chow, R. T.-P., 1983, On the Ability of Drops or Bubbles to Stick to Non-Horizontal Surfaces of Solids, *J. Fluid Mechanics*, 137: 1-29.
- Dussan V., E.B., 1985, On the ability of drops or bubbles to stick to non-horizontal surfaces of solids: Part 2. Small drops of bubbles having contact angles of arbitrary size, *J. Fluid Mech.* 151: 1-20.
- Elwing, H. et al. 1986, A Wettability Gradient Method for Studies of Macromolecular Interactions at the Liquid/Solid Interface, *Journal of Colloidal and Interface Science*, 119:203-210.
- Extrand, C.W., Gent, A.N., 1990, Retention of Liquid Drops by Solid Surfaces, *J. Colloid and Interface Sci.*, 138: 431-442.

- Extrand, C.W., Kumagai, Y., 1995, Liquid Drops on an Inclined Plane: The Relation Between Contact Angles, Drop Shape, and Retentive Force, *J. Colloid and Interface Sci.*, 170: 515-521.
- Feng, X.Q., Gao, X.F., Wu, Z.N., Jiang, L., Zheng, Q.S., 2007, Superior water repellency of water strider legs with hierarchical structures: Experimental and analysis. *Langmuir*. 23: 4892-4896.
- Fauvart, M., Phillips, P., Bachaspatimayum, D., Verstraeten, N., Fransaer, J., Michiels, J., Vermant, J., 2012, Surface tension gradient control of bacterial swarming in colonies of *Pseudomonas aeruginosa*. *Soft Matter*, 8: 70-76.
- Furstner R, Barthlott W, Neinhuis C and Walzel P, 2005, Wetting and self-cleaning properties of artificial superhydrophobic surfaces, *Langmuir* 21: 956-961.
- Jopp J, Grll H and Yerushalmi-Rozen R , 2004, Wetting behavior of water droplets on hydrophobic microtextures of comparable size, *Langmuir* 20:10015-10019.
- Larmour I, Bell S, Saunders G, 2007, Remarkably Simple Fabrication of Superhydrophobic Surfaces Using Electroless Galvanic Deposition. *Angewandte Chemie*. International Ed., 46:1710-1712.
- Oner, D., McCarthy, T.J., 2000, Ultrahydrophobic surfaces: effects of topography length scales on wettability, *Langmuir*, 16: 7777-7782.
- Puckorius, PR., Thomas, PT., Augsperger, R.L., 1995, The design and operation of evaporative coolers help prevent the growth and transmission of Legionnaires disease. *ASHRAE*: 29-3
- Sharma, CS, Abhiishek, K., Katepalli, H., Sharma, 2011, Biomimicked Superhydrophobic Polymeric and Carbon Surfaces, *Industrial & Engineering Chemistry Research*, 23: 13012-1320.
- Sommers AD, Jacobi, A.M., 2006, Creating microscale surface topology to achieve anisotropic wettability on an aluminum surface. *Micromech. Microeng.* 16:1571-1578.
- Vranken, RJ, Kusumaatmaja, H., Hermans, K., Prenen, AM. 2010, Fully reversible transition from Wenzel to Cassie-Baxter states on corrugated superhydrophobic surfaces. *Langmuir*. 26: 3335-3341.

### ACKNOWLEDGEMENT

The authors are grateful for financial support from a Research Incentive Grant at Miami University.